Dynamics of pulsed-ultrasound driven gas-liquid interfaces

Brandon Patterson & Eric Johnsen

Scientific Computing and Flow Physics Lab

University of Michigan, Ann Arbor

Department of Mechanical Engineering

Thursday June 29, 2017

Diagnostic ultrasound can trigger lung hemorrhage in mammals

- Lung Hemorrhage (LH) is the only known bioeffect of non-contrast DUS
- Has been shown to occur in mice, rats, pigs, rabbits, monkeys (Child *et al.*, 1990; O'Brien & Zachary, 1997; Tarantal & Canfield, 1994).
- The underlying physical damage mechanism is not understood.

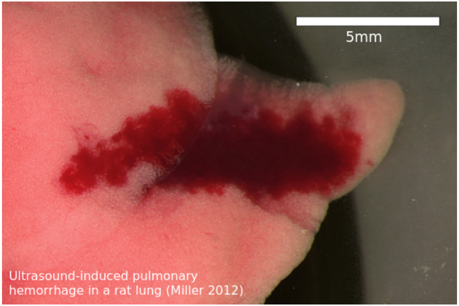

Ultrasound-induced pulmonary hemorrhage in a rat lung (Miller 2012)

Fundamental physical problem:

An acoustic wave interacting with a tissue-air interface

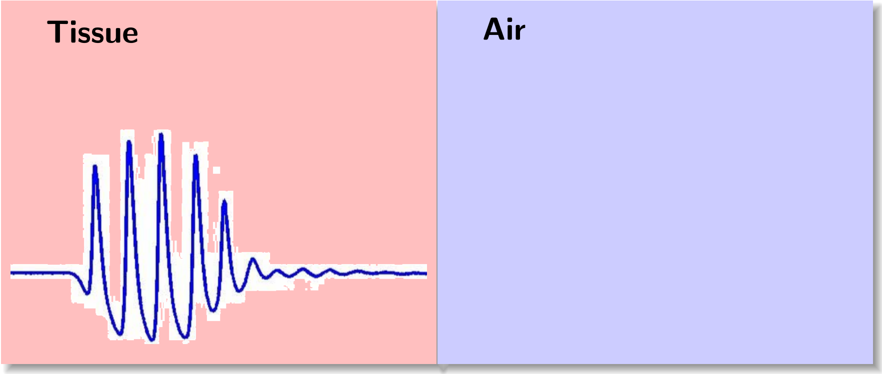

We want to understand the dynamics of this problem

Fundamental physical problem:

An acoustic wave interacting with a tissue-air interface

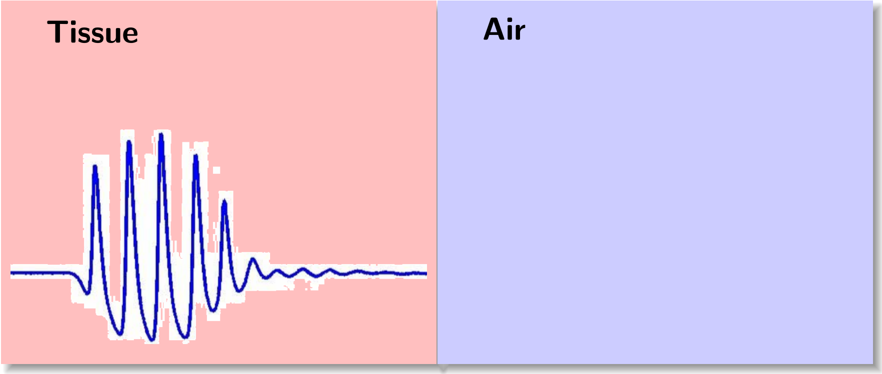

We want to understand the dynamics of this problem

Hypothesis:
Ultrasound waves generate baroclinic vorticity at gas-liquid interfaces, driving the interface deformation

Hypothesis:
Ultrasound waves generate baroclinic vorticity at gas-liquid interfaces, driving the interface deformation

Aims:

1. Test hypothesis
2. Simulate alveoli-like, gas-liquid interfaces driven by **clinically relevant** ultrasound waves
3. Calculate interface stresses and strains and compare with expected alveolar failure thresholds

Hypothesis:
Ultrasound waves generate baroclinic vorticity at gas-liquid interfaces, driving the interface deformation

Aims:

1. Test hypothesis
2. Simulate alveoli-like, gas-liquid interfaces driven by **clinically relevant** ultrasound waves
3. Calculate interface stresses and strains and compare with expected alveolar failure thresholds

Hypothesis:
Ultrasound waves generate baroclinic vorticity at gas-liquid interfaces, driving the interface deformation

Aims:

1. Test hypothesis
2. Simulate alveoli-like, gas-liquid interfaces driven by **clinically relevant** ultrasound waves
3. Calculate interface stresses and strains and compare with expected alveolar failure thresholds

We hypothesize that US waves generate baroclinic vorticity at gas-liquid interfaces, driving deformation.

- Air-tissue interfaces have sharp density gradients
- US has strong pressure gradients
- US-induced baroclinic vorticity may cause strain, similar to shock-driven interfaces
- Linear acoustics does not capture this.

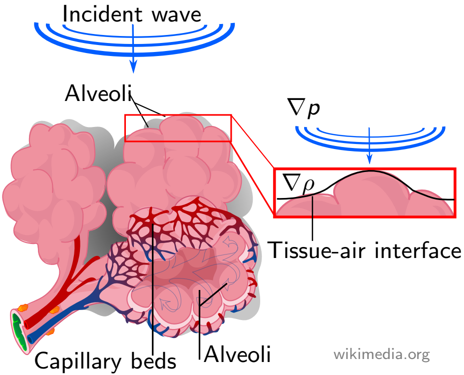

We hypothesize that US waves generate baroclinic vorticity at gas-liquid interfaces, driving deformation.

The vorticity generation equation

$$\frac{D\boldsymbol{\omega}}{Dt} = (\boldsymbol{\omega}\cdot\nabla)\,\mathbf{u} \quad -\boldsymbol{\omega}\,(\nabla\cdot\mathbf{u}) \;+ \frac{\nabla\rho\times\nabla p}{\rho^2} \;-\nabla\times\left(\frac{\nabla\cdot\boldsymbol{\tau}}{\rho}\right) \quad +\nabla\times\mathbf{B}$$

- Air-tissue interfaces have sharp density gradients
- US has strong pressure gradients
- US-induced baroclinic vorticity may cause strain, similar to shock-driven interfaces
- Linear acoustics does not capture this.

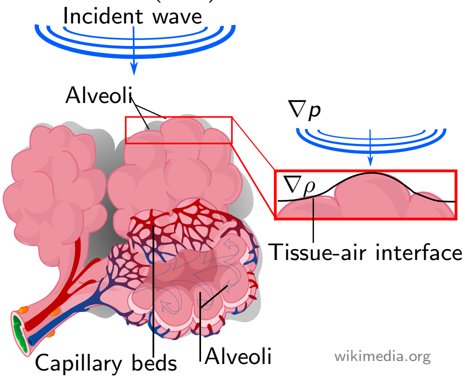

We hypothesize that US waves generate baroclinic vorticity at gas-liquid interfaces, driving deformation.

The vorticity generation equation

$$\frac{D\boldsymbol{\omega}}{Dt} = \cancelto{\mathcal{O}(0)}{(\boldsymbol{\omega}\cdot\nabla)\,\mathbf{u}} - \boldsymbol{\omega}\,(\nabla\cdot\mathbf{u}) + \frac{\boldsymbol{\nabla\rho\times\nabla p}}{\boldsymbol{\rho^2}} - \cancelto{\mathcal{O}(0)}{\nabla\times\left(\frac{\nabla\cdot\boldsymbol{\tau}}{\rho}\right)} + \cancelto{\mathcal{O}(0)}{\nabla\times\mathbf{B}}$$

- Air-tissue interfaces have sharp density gradients
- US has strong pressure gradients
- US-induced baroclinic vorticity may cause strain, similar to shock-driven interfaces
- Linear acoustics does not capture this.

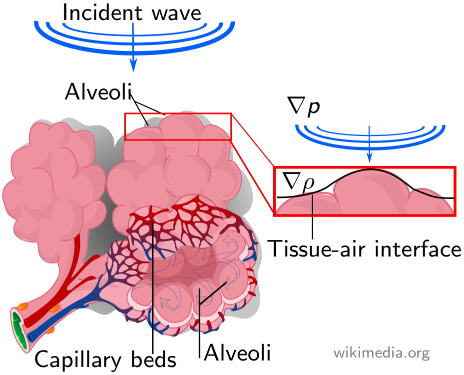

wikimedia.org

Past work: Acoustic waves are capable of deforming gas-liquid interfaces

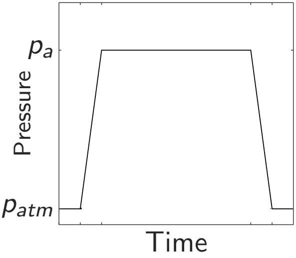

Input pressure

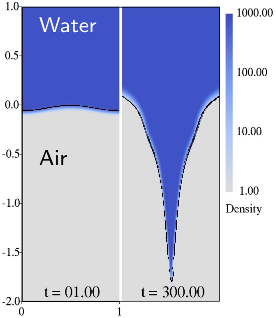

Density

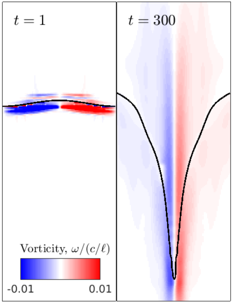

Vorticity

A trapezoidal acoustic waves caused significant deformations of an almost flat air-water interfaces. Linear acoustics couldn't explain this.

Patterson, B., & Johnsen, E. (2016). Dynamics of an acoustically driven liquid-gas interface. J. Acoust. Soc. Am.

Past work: Acoustic waves are capable of deforming gas-liquid interfaces

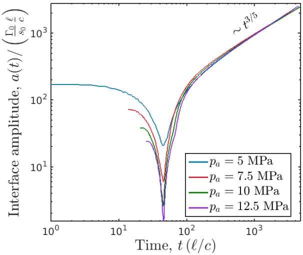

$a(t) \sim t^{3/5}$

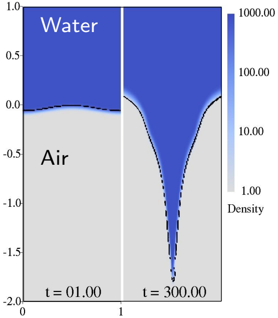

Density

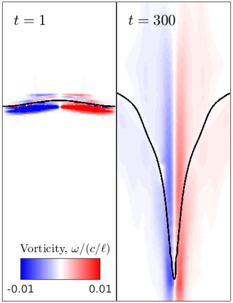

Vorticity

Interface deformation can be mathematically described in terms of vorticity, $\omega = \nabla \times \mathbf{u}$.

Patterson, B., & Johnsen, E. (2016). Dynamics of an acoustically driven liquid-gas interface. J. Acoust. Soc. Am.

Ultrasound driven alveoli are modeled as compressible fluids.

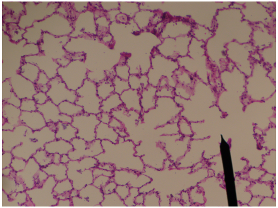

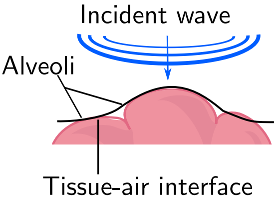

Physical problem schematic

Ultrasound driven alveoli are modeled as compressible fluids.

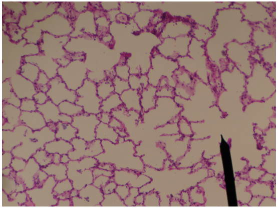

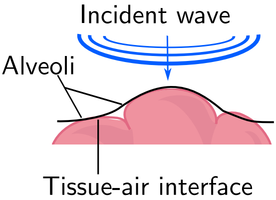

Physical problem schematic

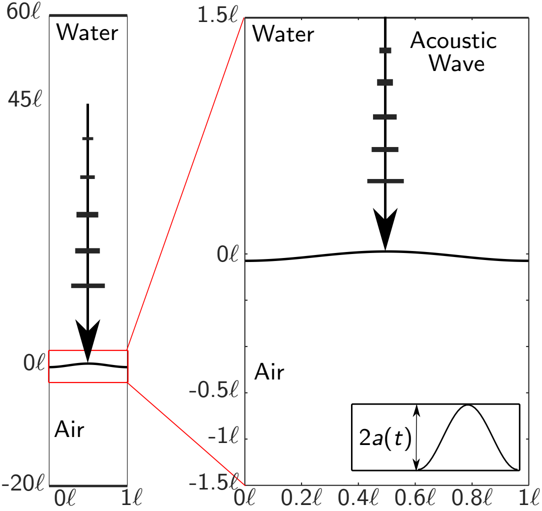

Domain and model problem schematic.

Ultrasound driven alveoli are modeled as compressible fluids.

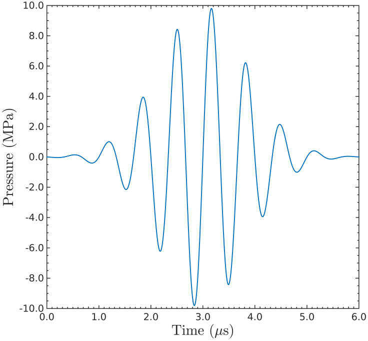

Ultrasound pulse waveform

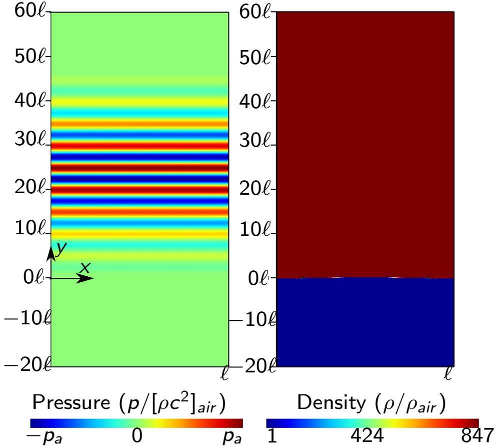

Initial Condition

The interface dynamics are simulated

Ex: Ultrasound pulse: $f = 1.5$ MHz, $p_a = 5$ MPa; Interface:$a_0 = 0.3\ell$.

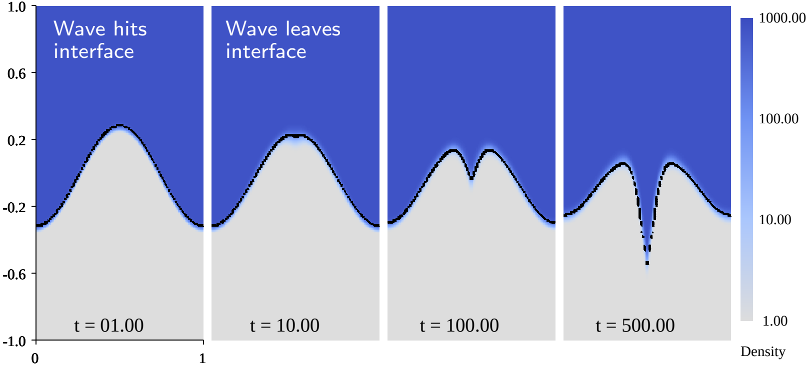

The interface evolves long after the wave has passed.

Linear acoustics can't explain this.

Hypothesis:
Ultrasound waves generate baroclinic vorticity at gas-liquid interfaces, driving the interface deformation

Aims:

1. Test hypothesis

Is the ultrasound-induced interface deformation driven by baroclinic vorticity?

Hypothesis:
Ultrasound waves generate baroclinic vorticity at gas-liquid interfaces, driving the interface deformation

Aims:

1. Test hypothesis

Is the ultrasound-induced interface deformation driven by baroclinic vorticity?

Baroclinic vorticity is driving the deformation after the wave passes

Consider an air-water interface driven by a 10 MPa ultrasound pulse

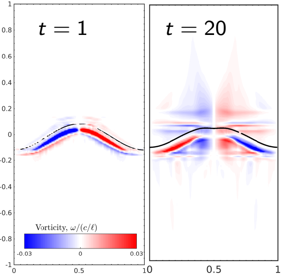

Vorticity

Interface amplitude grows as $\approx t^{3/5}$, at late times independently of the driving waveform

Baroclinic vorticity is driving the deformation after the wave passes

Consider an air-water interface driven by a 10 MPa ultrasound pulse

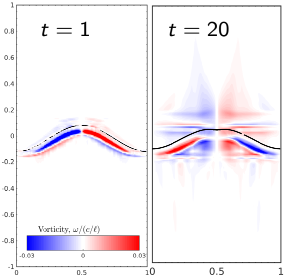

Vorticity

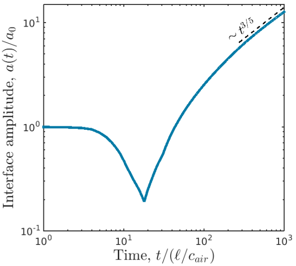

Interface growth $a(t)/a_0$

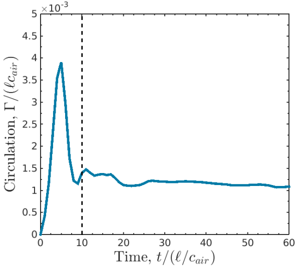

Circulation, $\Gamma = \int_{A_R} \omega dA$

Interface amplitude grows as $\approx t^{3/5}$, at late times independently of the driving waveform

Now let's consider the more clinically relevant cases

Wave and interface perturbation amplitudes are varied.

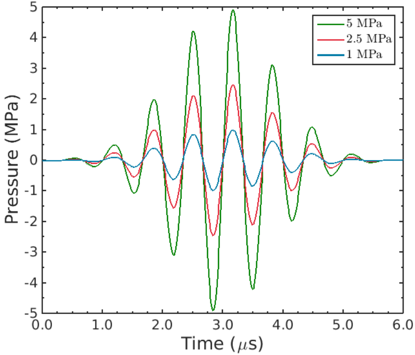

Ultrasound Pulses

- Assume typical alveolar diameter $\ell = 200\mu$m (Ochs *et al.*, 2004)
- Pulse amplitudes, $p_a = 1, 2.5, 5$ MPa; frequency, $f = 1.5$ MHz

Now let's consider the more clinically relevant cases

Wave and interface perturbation amplitudes are varied.

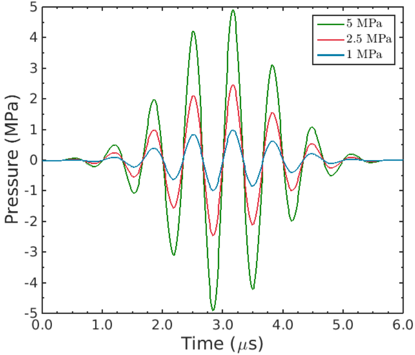

Ultrasound Pulses

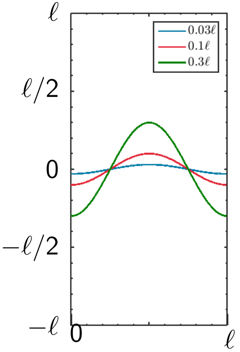

Interface initial conditions

- Assume typical alveolar diameter $\ell = 200\mu$m (Ochs *et al.*, 2004)
- Pulse amplitudes, $p_a = 1, 2.5, 5$ MPa; frequency, $f = 1.5$ MHz
- Interface perturbation amplitudes $a_0 = 0.03\ell, 0.10\ell, 0.30\ell$

The inferred viscous stress is calculated

$$\tau_{xy}(x,y,t) = \mu\left(\frac{\partial u}{\partial y} + \frac{\partial v}{\partial x}\right), \qquad p_a = 5\ \text{MPa}$$

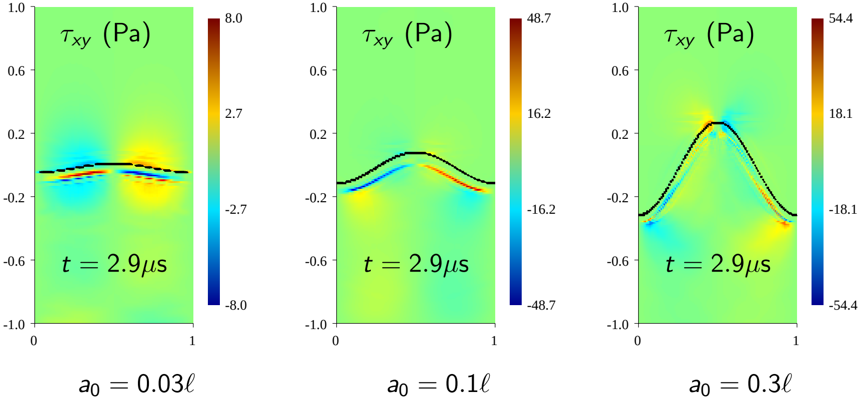

- Viscous shear stresses are concentrated at the interface
- The maximum shear stress, occurs approximately when the peak negative pressure hits the interface

The inferred viscous stress is calculated

$$\tau_{xy}(x, y, t) = \mu \left(\frac{\partial u}{\partial y} + \frac{\partial v}{\partial x} \right), \qquad a_0 = 0.3\ell \text{ MPa}$$

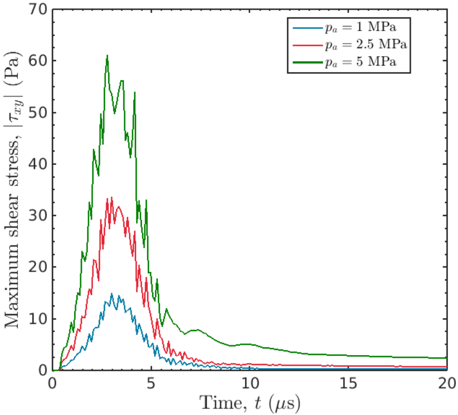

- Maximum calculated shear stress, ≈ 50 Pa
- $\approx$ alveolar wall stress failure criterion, 8 kPa (West *et al.*, 1991)

The interface strain is calculated

$$\varepsilon(t) = \frac{s(t)-s_0}{s_0}, \qquad s = \text{arclength of interface}$$

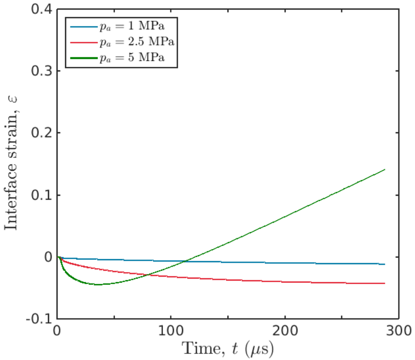

$a_0 = 0.1\ell$

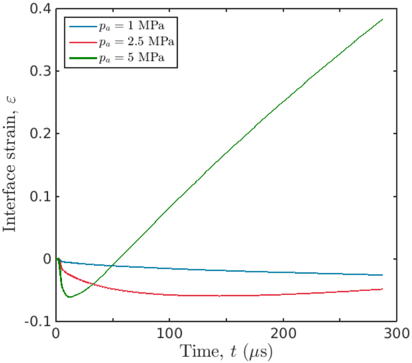

$a_0 = 0.3\ell$

- Strain increases with increasing p_a and a_0
- For $a_0 = 0.3\ell$ and $p_a = 1, 2.5$, and 5 MPa maximum strains, at $t \approx 300\mu$s, are $\varepsilon = -0.01, -0.05$, and 0.38 respectively.

Discussion and conclusions

- A single ultrasound pulse is sufficient to appreciably strain an air-water interface via baroclinic vorticity.
- Newtonian viscous stress alone is not likely to cause hemorrhage.
- Circulation from subsequent pulses could add up.
- Better characterization of mechanical properties (e.g, elasticity, viscosity) is needed.

Beyer, Robert T. 1974. *Nonlinear Acoustics*.

Child, S.Z., Hartman, C.L., Schery, L.A., & Carstensen, E.L. 1990. Lung damage from exposure to pulsed ultrasound. *Ultrasound med. biol.*, **16**(8), 817–825.

Miller, DL. 2012. Induction of Pulmonary Hemorrhage in Rats During Diagnostic Ultrasound. *Ultrasound med. biol.*, **38**(8), 1476–1482.

O'Brien, William D. W.D., & Zachary, J.F. 1997. Lung damage assessment from exposure to pulsed-wave ultrasound in the rabbit, mouse, and pig. *Ieee trans. ultrason. ferroelectr. freq. control*, **44**(2), 473–485.

Ochs, Matthias, Nyengaard, Jens R., Jung, Anja, Knudsen, Lars, Voigt, Marion, Wahlers, Thorsten, Richter, Joachim, & Gundersen, Hans Jørgen G. 2004. The Number of Alveoli in the Human Lung. *Am. j. respir. crit. care med.*, **169**(1), 120–124.

Tarantal, Alice F., & Canfield, Don R. 1994. Ultrasound-induced lung hemorrhage in the monkey. *Ultrasound med. biol.*, **20**(1), 65–72.

West, J B, Tsukimoto, K, Mathieu-Costello, O, & Prediletto, R. 1991. Stress failure in pulmonary capillaries. *J. appl. physiol.*, **70**(4), 1731–1742.

Governing Equations

Euler equations of fluid motion

$$\begin{aligned}
\frac{\partial \rho}{\partial t} + \frac{\partial(\rho u)}{\partial x} + \frac{\partial(\rho v)}{\partial y} &= 0,\\
\frac{\partial \rho u}{\partial t} + \frac{\partial}{\partial x}\left(\rho u^2 + p\right) + \frac{\partial}{\partial y}(\rho u v) &= 0,\\
\frac{\partial \rho v}{\partial t} + \frac{\partial}{\partial x}(\rho u v) + \frac{\partial}{\partial y}\left(\rho v^2 + p\right) &= 0,\\
\frac{\partial E}{\partial t} + \frac{\partial}{\partial x}\left[u(E+p)\right] + \frac{\partial}{\partial y}\left[v(E+p)\right] &= 0,
\end{aligned}$$

Stiffened equation of state

$$E = \frac{\rho\left(u^2+v^2\right)}{2} + \frac{p+\gamma B}{\gamma-1}.$$

Advection equations for γ, B prevent interface pressure oscillations.

$$\begin{aligned}
\frac{\partial}{\partial t}\left(\frac{\gamma B}{\gamma-1}\right) + u\frac{\partial}{\partial x}\left(\frac{\gamma B}{\gamma-1}\right) + v\frac{\partial}{\partial y}\left(\frac{\gamma B}{\gamma-1}\right) &= 0,\\
\frac{\partial}{\partial t}\left(\frac{1}{\gamma-1}\right) + u\frac{\partial}{\partial x}\left(\frac{1}{\gamma-1}\right) + v\frac{\partial}{\partial y}\left(\frac{1}{\gamma-1}\right) &= 0
\end{aligned}$$

A high-order accurate computational solution strategy is invoked

- An in-house developed code is used to solve the Euler equations.
- Numerical methods
  - 3^{rd} order Discontinuous Galerkin method is used in space
  - 4^{th} order Runge-Kutta time marching
  - Roe Solver used for element-to-element fluxes
- Acoustic waves are prescribed within the domain.
- Grid stretching reduces reflections.
- Grid size: $\ell \times 80\ell \, (L_x \times L_y)$

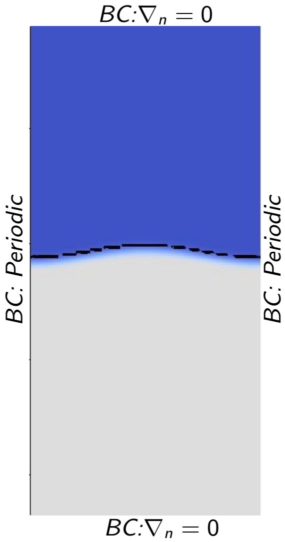

BACKUP SLIDES

Argument against viscosity - viscous length scales

$\nu_w = 0.7\ \mu\text{m}^2/\text{s}, \qquad \nu_a = 16.6\mu\text{m}^2/\text{s}, \qquad f_c = \mathcal{O}\left(10^6\right)\text{Hz}$

$\sqrt{\nu_{air}/f_c} = 4\mu\ \text{m} = \mathcal{O}\left(10^{-6}\right) << L_{\text{alveolus}} = \mathcal{O}\left(10^{-4}\right)$

$\sqrt{\nu_{air,ND}\,t} \approx 0.5 < a(t) - a_0 \approx 4$ at $t = 1000$

Therefore the scale of the viscous effect is smaller than the scale of the problem we are looking at, but may be important at late times.

Dimensional Numbers

- Let $\lambda_{alveolus} = 100\mu$ m, $u_0 = c_{air} = 343$ m, $v_0 =< \dot{a(t)} >\approx 0.65$ m/s, $u_{intf}(t = 20) = 12.8$ m/s, $G = 1$ kPa
- $\lambda_{alveolus} = 100\mu$ m, $u_0 = c_{air} = 343$ m, $v_0 =< \dot{a(t)} >\approx 0.65$ m/s
- $t = 1 \rightarrow t_{dim} = 0.292\mu$ s

Dimensionless Numbers

- $Fr = \frac{u_0}{\sqrt{g_0 \lambda}} \approx 11000$
- $Fr = \frac{v_0}{\sqrt{g_0 \lambda}} \approx 21$
- $Ca = \frac{\rho u_{intf}^2}{G_{Alv}} = 163$

Interface treatment

Interface thickness parameter:

$$\delta = 0.08\lambda$$

Normalized distance from interface:

$$d = \frac{\delta + y(x)_{interface} - y}{2\delta}$$

Volume fraction:

$$y_0 = \begin{cases} 1 \\ exp\left(log\left(10^{-16}\right)|d|^8\right) \\ 0 \end{cases}$$

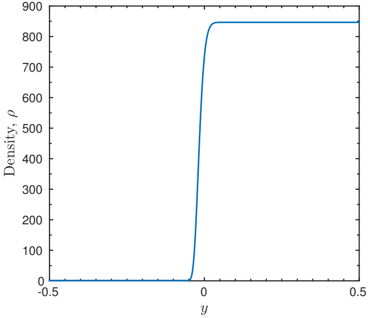

Radiation Pressure

$P_{net} = \frac{\Delta p_a}{2} \left[1 - \frac{c_w}{c_a} + \frac{(\rho c)_a - (\rho c)_w}{(\rho c)_a (\rho c)_w} \right]$ Beyer (1974)
Stress failure in the lungs:
Rabbit lungs under transmural pressure: $\approx 5.2kPa$ (West *et al.*, 1991);

Convergence tests: Compression wave

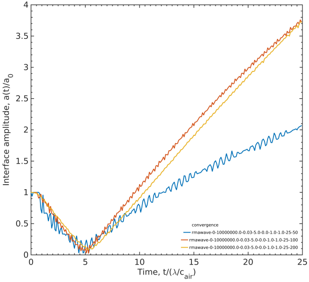

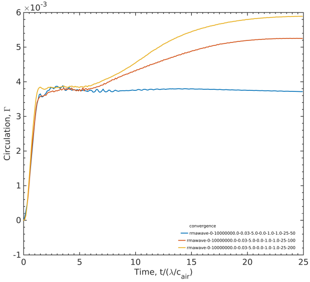

50 pts / λ, 100 pts / λ 200 pts / λ